World Journal of Advanced Research and Reviews

eISSN: 2581-9615 CODEN (USA): WJARAI

Cross Ref DOI: 10.30574/wjarr

Journal homepage: https://wjarr.com/

(Research Article)

Effect of dust storms on (GSM) signal north region of Libya

Braika Alameen [1], Sabriya Alghennai Alfitouri [2] and Abdussalam Ali Ahmed [3,*]

[1] *Department of Electric and Electronic Engineering, Bani Waleed University, Bani Walid/Libya.*
[2] *Department of Communications, College of Electronic Technology, Bani Walid, Libya.*
[3] *Department of Mechanical and Industrial Engineering, Bani Waleed University, Bani Walid, Libya.*

World Journal of Advanced Research and Reviews, 2022, 14(01), 504–519

Publication history: Received on 19 March 2022; revised on 28 April 2022; accepted on 30 April 2022

Article DOI: https://doi.org/10.30574/wjarr.2022.14.1.0351

Abstract

Propagation mechanisms are very complex and diverse, because of the separation between the receiver and the transmitter, attenuation (reduction or loss) of the signal strength occurs. Field study will be conducted in amid north region of Libya (Bani Walid), which has high wind speed, and high attenuation loss, desert climate, and frequent dust and sand storms. This phenomenon actually influenced on wireless communication systems (GSM signal), neither the effect of the humidity on the complex permittivity nor the antenna height on the visibility, where by its effect on both attenuation and cross-polarization constants in this region. Besides the expectation of different chemical analysis of the dust and sand. These samples were collected from five location, every location had one level and sand was collected from a height of 2m, collect the meteorological data for the region of this study, e.g. visibility, wind speed and relative humidity, and height of towers from Libyana technical station. The analysis of these samples were done in two laboratories, one in university of Tripoli (AL-Fateh University), and the second in the Industrial Research Center in Tripoli. In the analysis, we were looking for the chemical and physically composition, the chemical composition of dust and sand had been got to compute complex permittivity, density, and chemical and physical properties analysis for the samples. Determine equivalent diameter, particles-size distribution, and axes ratio for collected samples; determine equivalent diameter, particles-size distribution, and axes ratio for collected samples. Compute the attenuation loss and cross-polarization discrimination (XPD) change due to the effect of sand and dust storms on wireless communication systems (GSM signal) which coverage in the studied region.

Keywords: Attenuation loss; Humidity; Dust; Sand; Cross-polarization; Visibility

1. Introduction

The millimeter wave band provides the potential for more services than all of the lower radio bands together, unfortunately, the shorter the wavelength the more attenuation will be induced by absorption and scattering due to rain, dust and sand particles in the radio path. If the excess attenuation exceeds the available fade margin, the result is service interruption and system outage. For frequencies below 10 GHz, the common practice has been that the allowed outage time is allocated to equipment failure and fading. Excess attenuation due to hydrometers and other particles can be significant below 10 GHz, particularly in tropical areas. In the millimeter wave band, however, the practice was revised to allow more margins for rain and other effects induced attenuation. To meet reliability objectives, shorter hops must be used for moderate rain areas and wet regions, with shorter hops, most of the outage budget can be allocated to rain attenuation since significant refractive fading is less likely to occur on a short hop. In dry areas, marked by less than 200 mm of total rainfall per year, (as is the case for some parts of Libya) longer hops can be operated in the millimeter wave band with acceptable reliability. However, such areas are subject to frequent sand and dust storms during which particles of sand and dust may rise high enough above the ground to obstruct the radio beam either by

* Corresponding author: Braika Alameen
Department of Electric and Electronic Engineering, Bani Waleed University, Bani Walid/Libya

attenuating or by cross polarization. Such storms may last for minutes or days, reducing visibility to several kilometers or as little as a few meters [1].

"In the literature the particles with radii less than 60 micron termed clay or silt, and the dust used to refer to airborne particles with radii less than 60 micron. Airborne particles with radii greater than 60 micron maintain the name sand, these are the definitions used by [2]". Dust storms are frequently mislabeled as "sandstorms." these are two different phenomena, dust storms usually occur over arable land where there has been a drought over extended periods, strong winds may raise the fine surface particles, referred to as dust, as high as one kilometer. Hence, the fall speeds of such particles are such that the dust may obscure the sun for extended periods. To be classified as a dust storm, the visibility must be smaller than 1 km. When the visibility is shorter than 500 m, it is called a "severe dust storm" [2].

1.1. Samples Collection and Meteorological Data

The region of this study was chosen where there is a high potential of sand and dust storms, and a place where there are many wireless communication networks, it is located at the mid north of Libya between longitude (13.30 to 15 N) and latitude (13 to 32 E). It is the city of (Bani Walid).

1.2. The meteorological data

The college meteorological data was obtained for a period of 8-years (from 1998 up to the end of 2005), this data for the wind speed is in the table (2).In this table, the first number stands for the direction from which the wind is coming, while the second stands for the speed in a knot (1 knot=1.85 km/h). [4].The Relative humidity is in the table (1).

Table 1 Relative humidity for (Bani Walid)

YEAR	JAN.	FEB.	MAR.	APR.	MAY	JUN.	JUL.	AUG.	SEP.	OCT.	NOV.	DEC.
1998	95	97	96	100	100	100	100	98	96	98	96	99
1999	91	99	98	94	89	89	84	86	97	95	95	100
2000	100	100	100	100	100	95	95	100	95	100	100	94
2001	96	100	100	99	98	95	98	96	100	95	96	96
2002	100	97	95	95	95	94	96	95	100	98	98	98
2003	97	97	100	96	91	96	96	96	95	98	95	97
2004	98	97	97	99	97	97	96	91	96	93	95	100
2005	97	92	95	93	94	95	95	91	96	99	98	96

Table 2 Wind Speed for (Bani Walid)

Year	JAN.	FEB.	MAR.	APR.	MAY	JUN.	JUL.	AUG.	SEP.	OCT.	NOV.	DEC.
1998	330/15	250/17	360/30	100/30	240/20	030/20	240/20		300/18	060/15	350/20	240/25
1999	270/25	270/22	360/25	330/20	250/12	020/20	040/20	090/20	360/20	230/25	330/22	280/30
2000	300/25	330/25	210/27	240/40	090/25	360/25	360/30	150/25	210/30	060/28	180/25	350/30
2001	240/25	270/30	360/35	240/30	180/30	360/25	360/25	090/25	360/25	030/18	180/30	270/30
2002	360/25	360/30	300/28	150/35	240/40	360/29	180/28	240/32	060/20	240/25	270/33	270/28
2003	260/38	270/40	350/30	240/35	120/22	050/20	090/20	020/35	240/25	030/25	210/25	300/23
2004	300/35	240/30	360/30	360/25	240/30	180/30	030/20	090/20	030/22	240/20	260/28	210/25
2005	270/40	240/35	240/25	300/30	330/30	030/25	060/20	090/20	360/22	030/20	180/20	260/45

1.3. Samples of Dust and Sand

The samples were collected in the summer of 2009 from five locations; the sand was collected from a height of 2m from the surface of earth (above the roofs of the stations).

1.4. Chemical Composition

Industrial Research Center laboratory are given in Tables (3), (4), (5), (6) and (7).

Table 3 Chemical Analysis of location (1)

Test method	Location 1	Component
Text Book of Vogel	77.169	SiO_2 %
Text Book of Vogel	11.985	CaO %
Text Book of Vogel	2.029	MgO %
A.A.S	6.075	Al_2O_3 %
A.A.S	0.918	Fe_2O_3 %
Flame photometer	1.416	Na_2O %
Flame photometer	0.357	K_2O %
A.A.S	0.047	MnO_2 %

Table 4 Chemical Analysis of location (2)

Test method	Location 2	Component
Text Book of Vogel	81.421	SiO_2 %
Text Book of Vogel	11.629	CaO %
Text Book of Vogel	0.493	MgO %
A.A.S	4.382	Al_2O_3 %
A.A.S	0.839	Fe_2O_3 %
Flame photometer	1.000	Na_2O %
Flame photometer	0.197	K_2O %
A.A.S	0.034	MnO_2 %

Table 5 Chemical Analysis of location (3)

Test method	Location 3	Component
Text Book of Vogel	84.097	SiO_2 %
Text Book of Vogel	12.378	CaO %
Text Book of Vogel	0.4981	MgO %
A.A.S	1.9053	Al_2O_3 %
A.A.S	0.7471	Fe_2O_3 %
Flame photometer	0.2864	Na_2O %
Flame photometer	0.0622	K_2O %
A.A.S	0.0249	MnO_2 %

Table 6 Chemical Analysis of location (4)

Test method	Location 4	Component
Text Book of Vogel	79.7046	SiO_2 %
Text Book of Vogel	16.1979	CaO %
Text Book of Vogel	1.0230	MgO %
A.A.S	1.7706	Al_2O_3 %
A.A.S	0.6689	Fe_2O_3 %
Flame photometer	0.5508	Na_2O %
Flame photometer	0.0629	K_2O %
A.A.S	0.0209	MnO_2 %

Table 7 Chemical Analysis of location (5)

Test method	Location 5	Component
Text Book of Vogel	79.7046	SiO_2 %
Text Book of Vogel	16.1979	CaO %
Text Book of Vogel	1.0230	MgO %
A.A.S	1.7706	Al_2O_3 %
A.A.S	0.6689	Fe_2O_3 %
Flame photometer	0.5508	Na_2O %
Flame photometer	0.0629	K_2O %
A.A.S	0.0209	MnO_2 %

From table (3, 4, 5, 6, and 7) we get the major constituents of the sample as SiO_2, CaO

1.5. Density and Conductivity

Table 8 Density and Conductivity

Sample No.	Density(g/ml)	Conductivity(µs/cm)
1	1.145	34300
2	1.3025	37800
3	1.678	4300
4	1.5777	17660
5	1.2683	46100

The average density and conductivity at this level for the area can be considered as (1.3943g/ml) and average conductivity of (28032 µs/cm).

1.6. Particle-Size-Distribution for samples

Sands are most generally measured by sieving.

I Equipment:

1 set of sieves = 2. 36, 2. 00, 1. 18, 0. 600, 0. 425, 0. 300, 0. 212, 0. 150, 0. 125, 0. 090, 0. 063, 0. 038, pan (12 sieves and the pan)

Sieve shaker supplied in lab, Balance to measure mass of samples, Computer with a spread, sheet program

II Materials: Sand sample, large sheet of paper, smaller sheet of paper-notebook paper will do 12 containers to place sieved samples in; these can be weighing trays.

Probability graph paper with linear horizontal scale

From the results presented: A particle size distribution (PSD) can be displayed graphically as in figure (1) shows the relation between diameter of particle and cumulative weight (%).

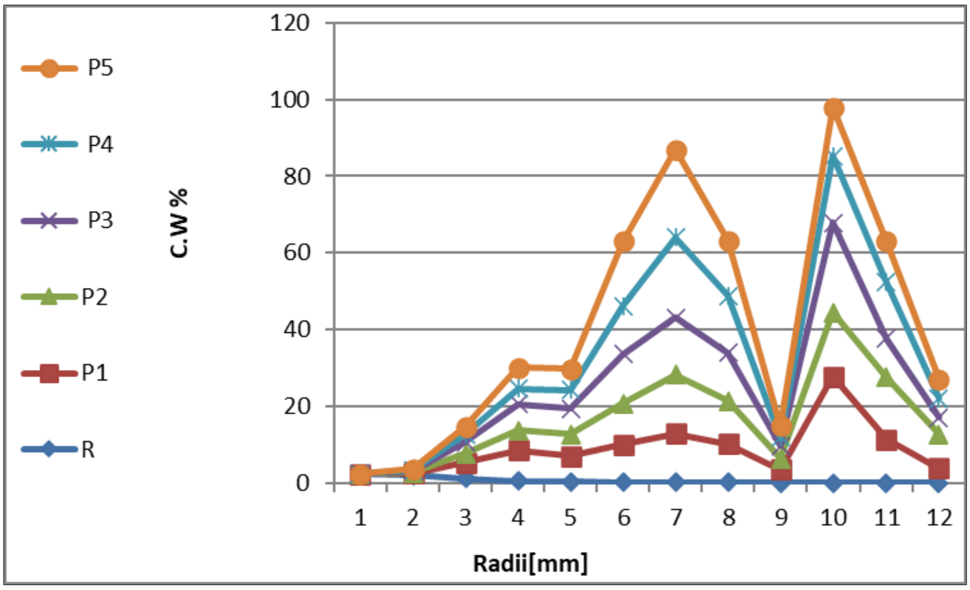

Figure 1 PSD of Samples

1.7. Calculation of dielectric constant for Samples

From the values of the dielectric constant, we can calculate the dielectric constant of mixture of (n) substances by using the looyenga equation as given by [3]

$$\epsilon_m 1/3 = \sum i \, \epsilon_i 1/3 \, V_i \quad (1)$$

Where:

ϵ_m is the complex dielectric constant of the mixture.

ϵ_i is the complex dielectric constant of the i^{th} substance.

V_i is the relative volume of the i^{th} sample from the volume of the total sample.

Using the results presented in Tables (1),(2),(3),(4),(5),(6),(7)and equation(1)we get the complex dielectric constants of a mixture using table(9) for the complex permittivity of each substance.

Table 9 Complex Permittivity of Substances

Compound	**complex permittivity**
SiO_2	4.43-j0.04
Al_2O_3	12.66-j1.31
Fe_2O_3	16.58-j0.93
$CaCO_3$	8.22-j0.12
$MgCO_3$	5.03-j0.17
$CaSO_4$	5.01-j0.08
MnO_2	75.74-j26.29

Using table (9) and equation (1) we get the results presented in tables (10), (11), (12), (13), (14) the dielectric constant of each sample.

Table 10a Analysis of Sample No (1)

Compound	$\varepsilon^{'} + j\varepsilon^{''}$	**V**	$\varepsilon^{1/3}V$
SiO_2	4. 43-j0. 04	0. 77169	1. 2674-j0. 0038
$CaCO_3$	8. 22-j0. 12	0. 11985	0. 2419-j0. 0012
$MgCO_3$	5. 03-j0. 17	0. 02029	0. 0348-j0. 0004
Al_2O_3	12. 66-j1. 31	0. 06075	0. 1418-j0. 0049
Fe_2O_3	16. 58-j0. 93	0. 00918	0. 0234-j0. 0004

The complex dielectric constant of the mixture is. ϵ_m =4.9928 – j0. 0937

Table 10b Results of (10a) after Normalization

Compound	$\varepsilon^{'} + j\varepsilon^{''}$	**V**	$\varepsilon^{1/3}V$
SiO2	4.43-j0.04	0.72994	1.1988 –j0.0036
CaCO3	8.22-j0.12	0.12203	0.2463-j0.0012
MgCO3	5.03-j0.17	0.02065	0.0354-j0.0004
Al2O3	12.66-j1.31	0.06185	0.1443-j0.0050
Fe2O3	16.58-j0.93	0.00934	0.0238-j0.0004

From equation (1) the complex dielectric constant of the mixture in this case

ϵ_m =4.4805- j0.0865

The average of the two will be:

1/2(4.9928 – j 0.0937 + 4.4805- j0.0865) =4.7367-j 0.0901

Table 11a the Analysis Sample No (2)

Compound	$\varepsilon' + j\varepsilon''$	V	$\varepsilon^{1/3}V$
SiO_2	4.43-j0.04	0.81421	1.3372-j0.0040
$CaCO_3$	8.22-j0.12	0.11629	0.2347-j0.0011
$MgCO_3$	5.03-j0.17	0.00493	0.0084-j0.0001
Al_2O_3	12.66-j1.31	0.04382	0.1023-j0.0035
Fe_2O_3	16.58-j0.93	0.00839	0.0214-j0.0004

From the table above and from equation (1) we get the complex dielectric constant of the mixture as ϵ_m =4.9476-j0.0799

Table 11b Results of (11a) after Normalization

Compound	$\varepsilon' + j\varepsilon''$	V	$\varepsilon^{1/3}V$
SiO_2	4.43-j0.04	0.82427	1.3538-j0.0041
$CaCO_3$	8.22-j0.12	0.11772	0.2376-j0.0012
$MgCO_3$	5.03-j0.17	0.00499	0.0086-j0.0001
Al_2O_3	12.66-j1.31	0.04436	0.1035-j0.0036
Fe_2O_3	16.58-j0.93	0.00849	0.0217-j0.0004

From the above and from the equation (1) the complex dielectric constant of the mixture as:

ϵ_m =5.1331-j0.0829

The average of the two values will be:

1/2(4.9476-j 0.0799+5.1331-j 0.0829) =5.0404-j 0.0814

Table 12a Analysis of Sample No (3)

Compound	$\varepsilon' + j\varepsilon''$	V	$\varepsilon^{1/3}V$
SiO_2	4.43-j0.04	0.84097	1.3812-j0.0042
$CaCO_3$	8.22-j0.12	0.12378	0.2498-j0.0012
$MgCO_3$	5.03-j0.17	0.004981	0.0085-j0.0001
Al_2O_3	12.66-j1.31	0.019053	0.0445-j0.0015
Fe_2O_3	16.58-j0.93	0.007471	0.0191-j0.0004

From the above table (12a) and equation (1) the complex dielectric constant of the mixture is ϵ_m = 4.9392-j0.0640

Table 12b Results of (12a) after Normalization

Compound	$\varepsilon^{'} + j\varepsilon^{''}$	**V**	$\varepsilon^{1/3}V$
SiO_2	4.43-j0.04	0.84411	1.3863-j0.0042
$CaCO_3$	8.22-j0.12	0.12424	0.2507-j0.0012
$MgCO_3$	5.03-j0.17	0.00499	0.0086-j0.0001
Al_2O_3	12.66-j1.31	0.01912	0.0446-j0.0015
Fe_2O_3	16.58-j0.93	0.00749	0.0191-j0.0004

From equation (1) the complex dielectric constant of the mixture in this case

ϵm =4.9943 –j0.0647 the average of the two will be:

½(4.9392-j0.0640 +4.9943 –j0.0647) =4.96675+j0.06435

Table 13a Calculated sand parameters No (4)

Compound	$\varepsilon^{'} + j\varepsilon^{''}$	**V**	$\varepsilon^{1/3}V$
SiO_2	4.43-j0.04	0.797046	1.3090-j0.0039
$CaCO_3$	8.22-j0.12	0.161979	0.3269-j0.0016
$MgCO_3$	5.03-j0.17	0.010230	0.0175-j0.0002
Al_2O_3	12.66-j1.31	0.017706	0.0413-j0.0014
Fe_2O_3	16.58-j0.93	0.006689	0.0171-j0.0003

From the table above and from equation (1) we get the complex dielectric constant of the mixture as:

ϵ_m =5. 0163-j0. 0656

Table 13b Results of (13a) after Normalization

Compound	$\varepsilon^{'} + j\varepsilon^{''}$	**V**	$\varepsilon^{1/3}V$
SiO_2	4.43-j0.04	0.80210	1.3173-j0.0040
$CaCO_3$	8.22-j0.12	0.16300	0.3290-j0.0016
$MgCO_3$	5.03-j0.17	0.01029	0.0176-j0.0002
Al_2O_3	12.66-j1.31	0.01781	0.0416-j0.0014
Fe_2O_3	16.58-j0.93	0.00673	0.0172-j0.0003

From the above and from the equation (1) the complex dielectric constant of the mixture as:

ϵ_m =5.1119-j0.669

The average of the two values will be:

1/2(5.0163-j0.0656+5.1119-j0.0669) =5.0641-j0.06625

Table 14a The Analysis Sample No (5)

Compound	$\varepsilon' + j\varepsilon''$	**V**	$\varepsilon^{1/3}V$
SiO_2	4.43-j0.04	0.796208	1.3077-j0.0039
$CaCO_3$	8.22-j0.12	0.139320	0.2812-j0.0014
$MgCO_3$	5.03-j0.17	0.010023	0.0172-j0.0002
Al_2O_3	12.66-j1.31	0.029056	0.0678-j0.0023
Fe_2O_3	16.58-j0.93	0.007993	0.0204-j0.0004

From the table above and from equation (1) we get the complex dielectric constant of the mixture as Єm =4.8626-j0.0707

Table 14b Results of (14a) after Normalization

Compound	$\varepsilon' + j\varepsilon''$	**V**	$\varepsilon^{1/3}V$
SiO_2	4.43-j0.04	0.81006	1.3304-j0.0040
$CaCO_3$	8.22-j0.12	0.14174	0.2861-j0.0014
$MgCO_3$	5.03-j0.17	0.01019	0.0175-j0.0002
Al_2O_3	12.66-j1.31	0.02956	0.0690-j0.0024
Fe_2O_3	16.58-j0.93	0.00813	0.0207-j0.0004

From the above and from the equation (1) the complex dielectric constant of the mixture as:

$Є_m$ =5.1206-j0.0744.

The average of the two values will be:

1/2(4.8626-j0.0707+5.1206-j0.0744) =4.9916-j 0.0726

The value of dielectric constant of all samples for results in Industrial Research Center Analysis from Tables (10a), (11a), (12a), (13a) (14a), as given by:

Table 15 Results of the Complex Permittivity of each Sample

Sample No.	**Type**	**Єm**
1	Sand	4.9928-j0.0937
2	Sand	4.9476-j0.0799
3	Sand	4.9392-j0.0640
4	Sand	5.0163-j0.0656
5	Sand	4.8626-j0.0707

The average complex permittivity all sample is:

$Є_m$= 4.9517-j0.0748

The normalized value of dielectric constant from Tables (10b), (11b), (12b), (13b), (14b) as given in Table (16).

Table 16 Results when the Sample is normalized

Sample No.	Type	Єm
1	sand	4.4805-j0.0865
2	sand	5.1331-j0.0829
3	sand	4.9943-j0.0647
4	sand	5.1119-j0.669
5	sand	5.1206-j0.0744

The average complex permittivity all sample is:

Єm= 4.9681 - j0.1955

2. Calculation of the Average Density for Samples

From the results presented the average density equal [1.3943(g/ml)] from the previous tables the following remakes, can be pointed out

- The average complex constant from table (15) equal to (4.9517-j0.0748)
- The average complex dielectric constant from table (16) equal to (4.9681 - j0.1955)
- The average complex dielectric constant from two approaches is ϵ_m=4.9599-j0.1351 and this could be used as the effective complex permittivity for the studied area of Libya (Bani-Walid)
- The average density equal to (1.3943(g/ml)) and this could be used as the effective average density for the studied are of Libya (Bani Walid).

3. Calculation of the Probability from PSD Analysis for samples

From the results: A particle size distribution (PSD) can be displayed graphically as in figure (2) shows the relation between the weight % and grain diameter (micron).

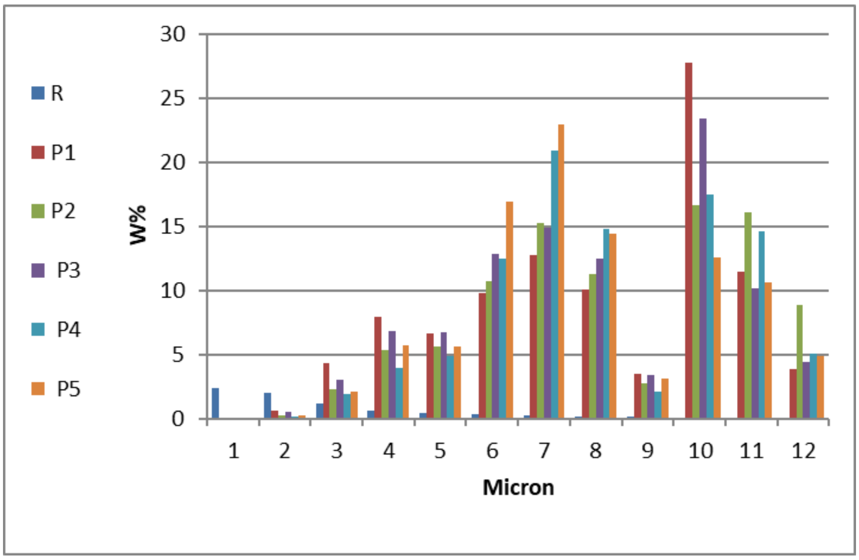

Figure 2 Graph Between the weight % and Grain Diameter (micron)

4. Estimating the visibility from meteorological data:

Meteorological data recorded for Libya lacks any information **about** the visibility, so we decided to estimate it by considering it inversely proportional to the wind speed, to find the constant of proportionality we depended on the visibility value.

$$\text{Visibility}=\frac{Constant}{Speed} \quad (2)$$

$$V=\frac{K}{S} \quad (3)$$

$$100=\frac{K}{30} \quad (4)$$

K = 3000

$$V_i=\frac{3000}{S_i} \quad (5)$$

Where:

V_i is the visibility in meters

S_i is the wind speed in knots.

Using the data provided to us by the metrological center in Tripoli for the wind speed data for e eight years we were able to estimate the visibility for the sites of concern for the months that has the highest wind.

Table 17 The Visibility in (Bani Walid)

Year	JAN.		FEB.		MAR.		APR.		MAY.		DEC.	
	S	**V**	**S**	**V**	**S**	**V**	**S**	**V**	**S**	**V**	**S**	**V**
1998	15	200	17	176.4	30	100	30	100	20	150	25	120
1999	25	120	22	136	25	120	20	150	12	250	30	100
2000	25	120	25	120	27	111	40	75	25	120	30	100
2001	25	120	30	100	35	85.7	30	100	30	100	30	100
2002	25	120	30	100	28	107	35	85.7	40	75	28	107
2003	38	78.9	40	75	30	100	35	85.7	22	136	23	130
2004	35	85.7	30	100	30	100	25	120	30	100	25	120
2005	40	75	35	85.7	25	120	30	100	30	100	45	66.6

The visibility for the six months during which the storms peak can be calculated using the data presented in Table (2), and using program (2) ,the visibility for these months are shown in Tables (17) from which we see that the lowest visibility was around 66.6 meter and it occurred on Dec 2005 , instead of using the visibility on a monthly basis we believe that working with the average visibility over the six months period along with the average speed is much better. This is as if we were using a fitting to the data before using it, the average speed along with the average visibility is given in Table (18) with this approach the minimum average visibility in (Bani Walid) was 91 meter.

Table 18 Average of Visibility in (Bani-Walid)

Year	Average	
V(m)	S (k)	
141	22.8	1998
146	22.3	1999
107.6	28.6	2000
100.9	30	2001
99	31	2002
100.9	31.3	2003
104	29	2004
91	34	2005

5. Height Towers in GSM network

Have a technical information about GSM stations (Libyana) located in study region. We note that the towers have height h= 12m , and we have one level to collect samples h0=2m ,.,and (f= 900MHz ,and f=1800 MHz).

6. Estimate of Air Relative Humidity

The complex permittivity depends on moisture contents in samples, S. M. Sharief [5] arrived at the following empirical relation for the variation of complex permittivity with relative humidity.

$$\varepsilon' = 5.52 + 0.04\mathrm{H} - 7.78\times10^{-4}\mathrm{H}^2 + 5.56\times10^{-6}\mathrm{H}^3 \quad (6)$$

$$\varepsilon'' = 0.16 + 0.02\mathrm{H} - 3.71\times10^{-4}\mathrm{H}^2 + 2.76\times10^{-6}\mathrm{H}^3 \quad (7)$$

6.1. Estimate of Air Relative Humidity for samples

We can use the equations (6) and (7) to estimate the effect of relative humidity on the complex permittivity in the studied area (Bani Walid), by changing the first term of both equations of the real part and imaginary part of complex permittivity of dry samples respectively as in equations below.

$$\varepsilon' = 4.9599 + 0.04\mathrm{H} - 7.78\times10^{-4}\mathrm{H}^2 + 5.56\times10^{-6}\mathrm{H}^3 \quad (6a)$$

$$\varepsilon'' = 0.1351 + 0.02\mathrm{H} - 3.71\times10^{-4}\mathrm{H}^2 + 2.76\times10^{-6}\mathrm{H}^3 \quad (7a)$$

1) For information based Libyana technical station and by using Є'& Є'' from table (15) and (16) are equal to 4.9599 and 0.1351 respectively.

ρ is the average measured density of the samples from table (8) is 1.3943 gm/m3, and by using program (1) ,the results are given in the following tables:

Table 19 Attenuation per km at Top of Tower [h_0=2m, h=12m, H=0%](dB/km)

Visibility at reference height(km)	**Att per Km at top of tower(dB/km)**	
	MHz900	**1800MHz**
0. 0522	0. 0002	0. 0003
0. 0563	0. 0002	0. 0003
0. 0710	0. 0001	0. 0002
0. 0938	0. 0001	0. 0002
0. 0992	0. 0001	0. 0002
0. 1000	0. 0001	0. 0002
0. 1010	0. 0001	0. 0002
0. 1070	0. 0001	0. 0002
0. 1255	0. 0001	0. 0001
0. 1303	0. 0001	0. 0001
0. 1360	0. 0001	0. 0001
0. 1400	0. 0001	0. 0001
0. 1446	0. 0001	0. 0001
0. 1500	0. 0001	0. 0001

Table 20 Attenuation per km at Top of Tower [h_0=2m, h=12m, H=50%] (dB/km)

Visibility at reference height(km)	**Att per Kmat top of tower(dB/km)**	
	MHz900	1800MHz
0.0522	0.0009	0.0017
0.0563	0.0008	0.0016
0.0710	0.0006	0.0013
0.0938	0.0005	0.0009
0.0992	0.0004	0.0009
0.1000	0.0004	0.0009
0.1010	0.0004	0.0009
0.1070	0.0004	0.0008
0.1255	0.0003	0.0007
0.1303	0.0003	0.0007
0.1360	0.0003	0.0006
0.1400	0.0003	0.0006
0.1446	0.0003	0.0006
0.1500	0.0003	0.0006

Table 21 Attenuation per km at Top of Tower [h0=2m, h=12m, H=100%] (dB/km)

Visibility at reference height(km)	Att per Km at top of tower(dB/km)	
	MHz900	1800MHz
0. 0522	0 .0 015	0. 0031
0. 0563	0. 0014	0. 0028
0. 0710	0. 0011	0. 0022
0. 0938	0. 0008	0. 0016
0. 0992	0. 0008	0. 0015
0. 1000	0. 0008	0. 0015
0. 1010	0. 0008	0. 0015
0. 1070	0. 0007	0. 0014
0. 1255	0. 0006	0. 0012
0. 1303	0. 0006	0. 0011
0. 1360	0. 0005	0. 0011
0. 1400	0. 0005	0. 0011
0. 1446	0. 0005	0. 0010
0. 1500	0. 0005	0. 0010

Figures (3) and (4) showing the relation between attenuation per km and visibility at reference height in the region of study (h0=2m, h =12m, for humidity 0%, 50%and100%)

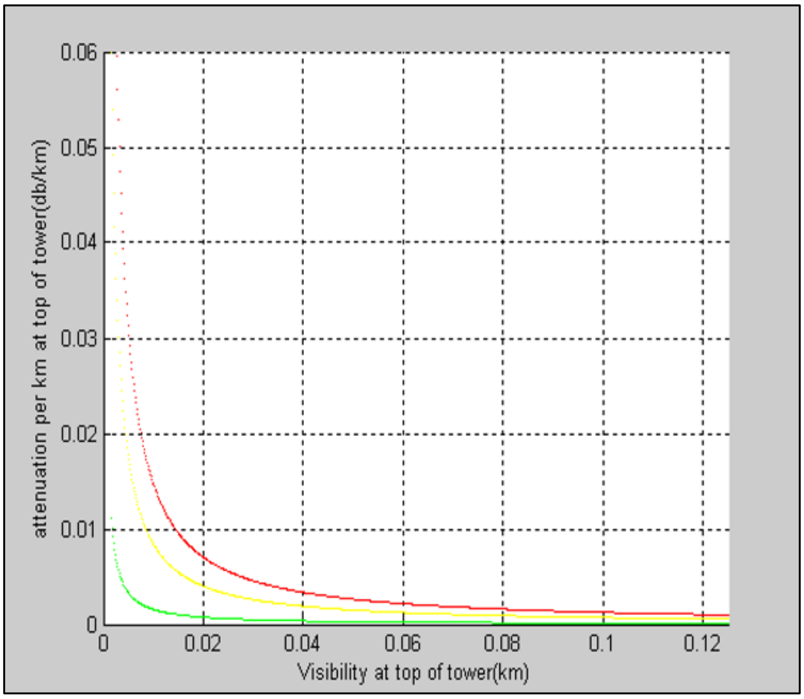

Figure 3 Attenuation per km at reference height and h0=2m, h=12m for f=900MHz

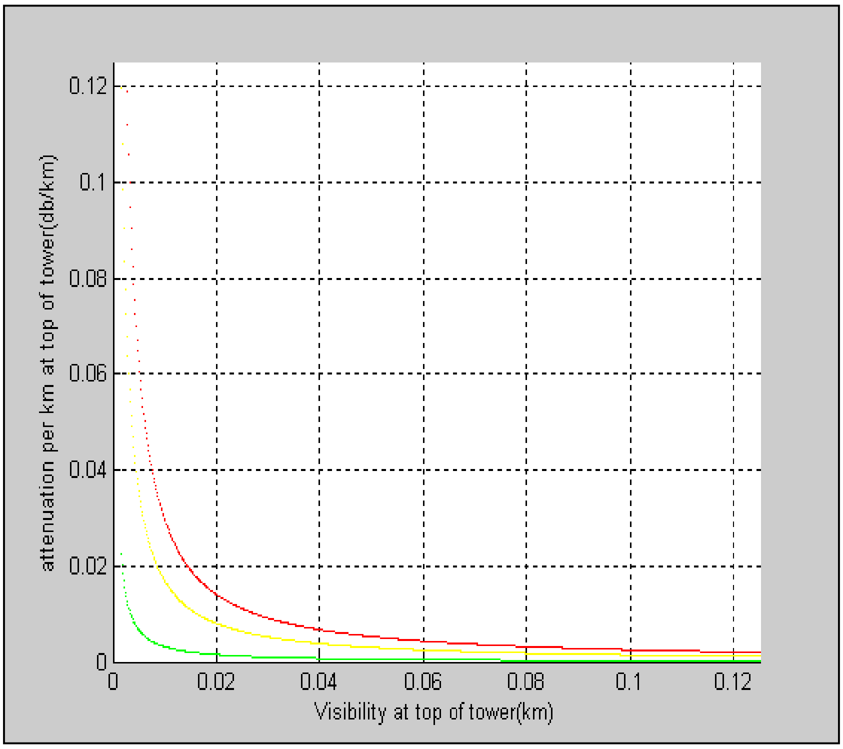

Figure 4 Attenuation per km at reference height and h0=2m, h=12m for f= M1800Hz

7. Estimation of the Cross-Polarization Constant

From size analysis of dust samples which was done in laboratories of the Libyan Petroleum Institute in Tripoli , it showed that some particles of all samples which photographed by using a special camera were mostly spherical in shape as shown in figure (5), and the axis ratios of particles are equal .

For spherical particles the attenuation and phase shift constants for both vertically polarized wave and horizontal polarized wave are equal, where by XPD becomes Infinite. Therefore, we conclude that the cross-polarization is not serious in microwave links of studding region, because shape of dust particles is spherical

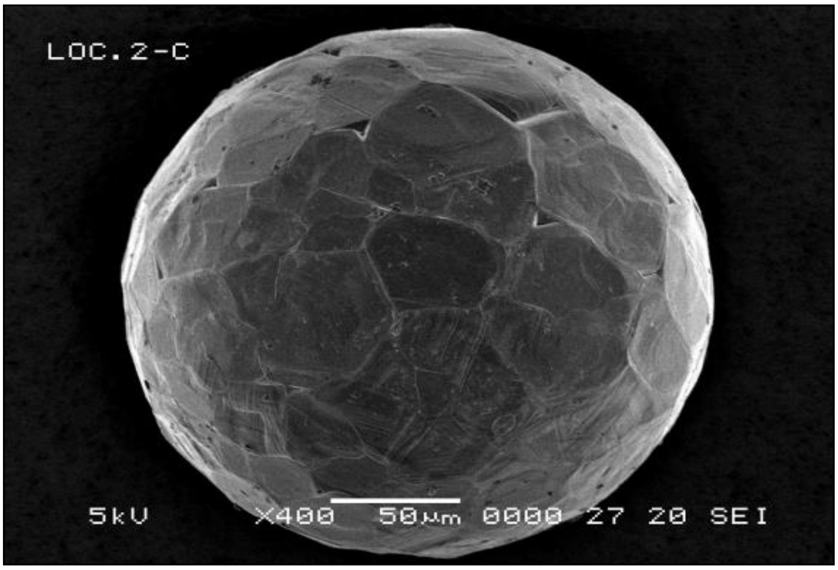

Figure 5 photograph of sample.

8. Discussion

From the previous tables the following summary of results can be pointed out:

- The chemical composition of all samples in the region of study comprises of over 85% of Sio2 by weight, so the Silicon dioxide has the greatest effect on the dielectric constant.
- The major constituents of samples are SiO , CaO.
- The average density of dry soil in studied region are equals to 1.03943gm/m^3, which depend on the constituents of samples.
- The average of complex permittivity of dry soil in the region of study are equal to 4.9549-j0.1351.
- The cross-polarization is not serious on microwave links of the region of study, because the shape of dust particles is spherical.

9. Conclusion

It was found through this study that presented the effect of dust storms on (GSM) signal north region of Libya that the average of complex permittivity of dry soil in amid north part of Libya (Bani Walid) for study equals to (4.9549-j0.1351), the average density of dry soil in the studied region equals to (1.3943gm/m3), over 70% of the samples have a diameter between (63-300μm), therefore the dominant grain size is sand. The cross-polarization is not serious in the wireless communication systems in the region of study, because the shape of dust particles is spherical.

Compliance with ethical standards

Disclosure of conflict of interest

The authors declare no competing interests.

References

[1] Hassan Aldeeb, ''Sand and Dust Storms Effects on Microwave Links, case study Agedabia –Jalo region '', Ms. c. Thesis, Altahadi University, Sirte- Libya, 2007.

[2] SI Ghobrial SM Sharief, "Microwave attenuation and cross polarization in dust storms," IEEE Trans. Antennas Propagat. , Apr. 1987; AP-35: pp. 418–425.

[3] Nafati Abdasallam Aboserwal, Microwave Attenuation and Cross Polarization Due To Dust Storms, Case Study Abo-Njeem"MSc 2 Thesis, University of AlFateh- Libya, 2008.

[4] Meteorological data from the weather watch in Tripoli- Libya.

[5] Sami M. Sharif, ''Clutter and backscatter cross-section of dust storms at x- band'', Sudan engineering society journal, June 1997; Vol. 44: No. 35.